The lithium ion conductor β-spodumene: an orientational glass

R. Böhmer*, P. Lunkenheimer, M. Lotze, A Loidl

Institut für Festkörperphysik, Technische Hochschule, D-64289 Darmstadt, Germany

Abstract. Polycrystals of β-spodumene were investigated using impadence spectroscopy for frequencies 0.1 Hz $< \nu <$ 235 GHz and for temperatures 5 K $<$ T $<$ 500 K. At high temperatures the Li ions are mobile and lead to dc and ac conductivity phenomena. These are analyzed in terms of the universal dielectric response and using the modulus formalism. The results obtained by both procedures are critically compared. At low temperatures or very high frequencies dielectric loss due to a dipolar freezing process is observed which bears a close resemblance to an orientational glass transition. To further confirm the glassy character of β-spodumene, we report measurements of the low temperature specific heat (3 K $<$ T $<$ 50 K) which provide evidence for the existence of excess contributions that are usually observed in amorphous materials.

1. Introduction

Spodumene, $LiAlSi_2O_6$, belongs to the small class of crystals that exhibit a contraction of certain crystallographic axes upon heating. The negative thermal expansion coefficient has technological relevance and is for instance used in "zero" expansion materials [1], it is due to the peculiar network structure which is built up from an array of corner-sharing SiO_4 and AlO_4 tetrahedra. This structure is similar to that of keatite which itself is a modification of quartz [2]. In β-spodumene the centers of the tetrahedra are however occupied randomly by Al^{3+} or by Si^{4+} and, to keep the charge balance, the network is "stuffed" by Li^+ ions which occupy interstitial sites.

The structure of β-spodumene involves 5, 7, and 8 membered rings of the SiO_4 and AlO_4 units which are partially interlocked. Their (rather complex) geometrical arrangement has been described in detail by Li and Peacor [2]. Since in the present investigation we are mainly interested in the dynamics of the Li^+ ions we show a simplified representation of the tetragonal unit cell of β-spodumene in Fig. 1 focusing only on the possible Li positions. It is seen that eight interstitial sites are available in the unit cell which contains four Li ions. These eight sites form four pairs with a lateral (center to center) distance of D = 4.75 Å [2]. The relevant distance within each double site is only d = 1.35 Å which is too short to be occupied by two Li^+ ions (radius 0.65 Å) at the same time.

As we will show in the present article this peculiar structure allows the observation of two rather different phenomena, viz. long-range ionic transport *and* freezing in the interstitial double sites, in the same crystal, albeit at different temperatures.

At high temperatures ion conduction processes are dominant, which have been investigated previously by electrical conductivity measurements and by ^{7}Li NMR experiments [3]. We monitor the motions of the mobile ions by broad-band impedance spectroscopy. The results obtained by this kind of technique are usually interpreted in terms different empirical formalisms by different authors. [4] The most commonly used approaches are based on the representation of the impedance data in terms of the electrical conductivity [5, 6, 7, 8] or in terms of the electrical modulus [9, 10]. These two ways of looking at ones data continue to provoke controversial discussions [11–14]. Therefore we have analyzed our data using both approaches which we then compare critically.

At low temperatures (or very high frequencies) long range ionic transport is ineffective, i.e. there is no exchange of ions between the paired sites. Thus each interstitial double site carries a well defined dipole moment $\mu = ed/2 = 3.25$ Debye (where e is the charge of the Li ion) which reverses its orientation if the ion hops. Anticipating one result of this article, the dipolar interaction between these moments or pseudo-spins however is not sufficiently strong to lead to the formation of an electrically ordered low temperature state.

**Present address*: Institut für Physikalische Chemie, Johannes Gutenberg-Universität, D-55099 Mainz, Germany (Tel.: + 49-6131-392536, Fax: + 49-6131-394196)

The disordered low temperature state of crystalline systems that emerges from an interaction dominated freezing of pseudo-spins, is usually termed orientational glass (OG). [15, 16] OG, like the structural glasses, exhibit the well known anomalies in quantities such as the specific heat, thermal conductivity, acoustic and electric absorption etc. [17] In order to confirm the glassy character of β-spodumene, in addition to impedance spectroscopy, we have carried out calorimetric measurements.

The present investigation of β-spodumene is part of an ongoing research program devoted to the study of ionic motions in lithium aluminosilicates. [18, 19, 20] For the present work we have used polycrystalline samples, since a study on single crystals has revealed that the conductivity of β-spodumene is isotropic [21].

The remainder of this paper is organized as follows: In the next section we give an overview of several theoretical concepts relevant to the description of the results obtained in this work. In Sect. 3 the experimental details are described very briefly. In Sect. 4.1 and 4.2 we present and analyze the dielectric results obtained on β-spodumene, in the high- and low-temperature regimes, respectively. Section 5 is devoted to a discussion of various aspects related to the local freezing of the Li-ions, i.e. to the orientational glass transition, as well as to a critical assessment of the various procedures employed to analyze ionic conduction processes. Finally in Sect. 6 the conclusions drawn from the present investigation are summarized.

2. Theoretical considerations

In this section we will summarize some concepts used to describe the temperature and frequency dependence of quantities related to the ionic conductivity σ and the dielectric constant ε. In the following section we will briefly discuss the temperature dependence of σ due to ion hopping. Then also the frequency dependence of the transport coefficients will be examined: in Sect. 2.2 with emphasis on the electrical conductivity and in Sect. 2.3 on the electrical modulus. Subsequently we will deal with aspects relevant for the analysis of the dielectric relaxation process found in β-spodumene at low temperatures. In Sect. 2.4 we will consider the effects of the dipolar interactions among the pseudo-spins associated with the Li-positions in the aluminosilicate lattice. The disorder present in the Li-sublattice can give rise to a broad distribution of relevant energy scales which can be obtained using the scaling procedure outlined in Sect. 2.5.

2.1. Thermally activated charge transport

The charge transport in most (but not all [22]) solid state ionic conductors proceeds in a thermally activated fashion. $\sigma \propto (n/T)\exp(-B/k_BT)$, n is the charge carrier density. Now we can define an effective conductivity relaxation rate ω_{eff} through $\sigma \propto n\omega_{eff}$ with $1/\omega_{eff} \propto T\exp(B/k_BT)$. Since the temperature dependence due to the exponent is much stronger than that due to the pre-exponent, one usually drops the prefactor and thus writes $\omega_{eff} = \omega_0 \exp(-B/k_BT)$.

The applicability of this equation to the case of ionic conductors is surprising for a number of reasons. The Arrhenius equation is conventionally derived under the implicit assumption that the jumps of different ions are independent from one another, a condition that in view of the relatively high density of lithium ions in β-spodumene is hardly met [23]. An inclusion of interaction effects requires more sophisticated treatments [24] which recently have been attempted using effectively one dimensional models [25]. Furthermore the disorder in the Al/Si sublattice can be expected to lead to a barrier distribution which is at least bimodal, still neglecting the possibility that a one-dimensional model may not be adequate to describe an isotropic conductor.

2.2. dc and ac conductivity

The complex conductivity $\sigma = \sigma' + i\sigma''$ of ionic and electronic conductors has often been expressed by the empirical relationship [6] which sometimes is called the universal dielectric response [7]

$$\sigma'(\omega) = \sigma_{dc} + A\omega^s. \tag{1a}$$

$$\sigma''(\omega) = \varepsilon_\infty \varepsilon_0 \omega + A\omega^s \tan(s\pi/2). \tag{1b}$$

Here ε_0 is the permittivity of free space and ε_∞ is the high-frequency dielectric constant. σ_{dc} denotes the dc part of the conductivity and the other terms are due to ac contributions. The separation of the conductivity into two (apparently independent) terms is somewhat artificial. [4] However, Eq. (1) is often a good approximation also to the results of more microscopic treatments, like e.g. in the random free energy model [8]. This model yields $\sigma(\omega) \propto i\omega\tau/\ln(1 + i\omega\tau)$, an expression which obviously cannot be split into additive ac and dc conductivity terms.

According to Almond and West [5], the prefactor appearing in Eq. (1) can be written as $A = \sigma_{dc}/\omega_c^s$. Thus one has

$$\sigma'(\omega) = \sigma_{dc}[1 + (\omega/\omega_c)^s], \tag{2}$$

with a conductivity relaxation rate, ω_c, that can be obtained from the condition $\sigma'(\omega_c) = 2\sigma_{dc}$. It is commonly found that ω_c is thermally activated

$$\omega_c \propto \exp(-B/k_BT). \tag{3}$$

If the carrier density n is also thermally activated, $n \propto \exp(-E_n/k_BT)$, as e.g. implied by weak electrolyte models, [26] the dc conductivity is written as

$$\sigma_{dc} \propto \exp[-(B + 2E_n)/k_BT]. \tag{4}$$

If the well known BNN relation [27] $\sigma_{dc} \sim \omega_c$, holds, one concludes that $E_n = 0$ [28]. This means that n is temperature independent. In this case the temperature dependence of the prefactor A is given by $A \propto \exp[B(1 - s)/k_BT]$. Hence for temperature invariant s, the ac conductivity is thermally activated with a barrier $B_{ac} = (1 - s)B$.

2.3. Relaxation processes

The motion of ionic charges in the sample has often been monitored either by determining the dielectric constant

ε or the electrical modulus M [29]. Dealing with the dielectric constant first, it is noted that it is measured by varying the electrical field applied to the sample and detecting the changes of its polarization P (or, more precisely, the dielectric displacement). In the frequency domain one can write the complex dielectric constant as

$$\varepsilon(\omega) = \varepsilon'(\omega) - \mathrm{i}\varepsilon''(\omega) \;=\; \varepsilon_\infty + \Delta\varepsilon \int \frac{g(\tau)\mathrm{d}\tau}{1 + \mathrm{i}\omega\tau}. \tag{5}$$

Here $\Delta\varepsilon \equiv \varepsilon_S - \varepsilon_\infty$ is called the dispersion strength, and $g(\tau)$ is a normalized distribution of relaxation times τ. In the time domain, one can measure a relaxation function $\phi(t)$ [= P(t)] subsequent to stepping an externally applied electric field

$$\phi(t) = \int_0^\infty g(\tau)\mathrm{e}^{-t/\tau}\mathrm{d}\tau. \tag{6}$$

This equation is obtained from Eq. (5) by Fourier transformation. The average dielectric relaxation time can be calculated from $g(\tau)$ or from $\phi(t)$ by using the following expression

$$\langle\tau_\varepsilon\rangle = \int_0^\infty \tau g(\tau)\,\mathrm{d}\tau \;=\; \int_0^\infty \phi(t)\,\mathrm{d}t \tag{7}$$

The description in terms of Eqs. (5) and (6) is most appropriate for the characterization of dipolar reorientation processes, for which variations in the dipole orientation obviously lead to variations of the polarization. The proper description of the transport of charge carriers however continues to constitute a matter of controversy. One familiar presentation of these processes is in terms of the complex conductivity.

$$\sigma(\omega) = \mathrm{i}\omega\varepsilon_0\varepsilon(\omega) \tag{8}$$

or in terms of the electrical modulus [9] M which formally may be viewed as the inverse dielectric constant.

However, the use of the modulus M corresponds to a different experimental situation in which, for a time domain experiment, the dielectric displacement D (or the amount of surface charge) is changed in a step like fashion and then kept constant. The step in D leads to an immediate built-up of an electrical field in the sample which decays with an average retardation time, $\langle\tau_M\rangle$, due to ionic motion. The decay of the electrical field may be described by a retardation function $\Phi(t) \propto E(t)$

$$\Phi(t) = \int_0^\infty G(\tau)\,\mathrm{e}^{-t/\tau}\,\mathrm{d}\tau, \tag{9}$$

where $G(\tau)$ is a distribution of retardation times. Fourier transformation of $-\mathrm{d}\Phi(t)/\mathrm{d}t$ yields for the complex frequency dependent modulus

$$M(\omega) = M'(\omega) + \mathrm{i}M''(\omega) \;=\; M_\infty \int \frac{\mathrm{i}\omega\tau G(\tau)\,\mathrm{d}\tau}{1 + \mathrm{i}\omega\tau.} \tag{10}$$

The detailed shape of the frequency dependent quantities M or ε (and σ) can either be specified by the distribution functions or likewise by the response function $\theta(t)$, i.e. $\phi(t)$ or $\Phi(t)$, and also by expressions such as Eq. (1). In most ionic conductors the imaginary part of the modulus exhibits a peak when plotted versus frequency. The peak is located at $\omega_p = 1/\tau_\sigma = \sigma_{dc}/(\varepsilon_\infty\varepsilon_0)$. In case σ' and ε' are frequency dependent the peak is broadened which usually is described in terms of a distribution of retardation times. In the modulus formalism τ_σ is termed conductivity relaxation time and usually is associated with a characteristic time scale for the motion of the ions. The temperature dependence of ω_c can then be identified with ω_{eff} as defined in Sect. 2.1. It is often found that the peak in M'' is located at a frequency where $\sigma'(\nu)$ changes from constant to power law behavior, i.e. in the vicinity of ω_c.

The imaginary part of the modulus is written as $M'' = \varepsilon''/(\varepsilon'^2 + \varepsilon''^2)$. Therefore, since $\varepsilon'^2 + \varepsilon''^2$ is practically constant at high frequencies, Eq. (1) together with Eq. (8) yields for this case

$$M''(\omega) \approx \varepsilon''(\omega) = \frac{1}{\varepsilon_0\omega} \lim_{\omega\to\infty} (\sigma_{dc} + A\omega^s) = \frac{A\omega^{s-1}}{\varepsilon_0}. \tag{11}$$

The transform $\int[-\mathrm{d}\theta(t)/\mathrm{d}t]\sin\omega\mathrm{d}t \propto M'' \approx \varepsilon''$ of one of the most popular expressions for the description of response functions [30] the Kohlrausch function $\theta(t) = \exp[-t/\tau)^\beta]$, yields a high frequency power law, $\omega^{-\beta}$, too. These considerations suggest the correspondence $\beta = 1 - s$, between the exponents which will be checked in the experimental sections, below.

2.4. Dipolar interactions: order and disorder

In order to estimate the energy scales relevant for the low-temperature freezing of the Li ions, we will in a first step focus on the dipolar interactions among the moments or pseudo-spins associated with the off-center positions of these ions in their interstitial sites. Then we will also take into account the disorder in the Al/Si sublattice. In Fig. 1 we show, in a schematic fashion, one out of the 2^4 ordered configurations of the 4 dipoles in the unit cell. The corresponding positions R_i and orientations $\boldsymbol{\mu}_i$ of the dipole moments are given in Table 1. The interaction energy between two (arbitrarily oriented) dipoles $\boldsymbol{\mu} = \mu_{eff}\hat{\mu}$ is given by

$$J_{ij} = \frac{\mu_{eff}^2}{r_{ij}^3}[\hat{\mu}_i\hat{\mu}_j - 3(\hat{\mu}_i\hat{r}_{ij})(\hat{\mu}_j\hat{r}_{ij})], \tag{12}$$

where $\mathbf{r}_{ij} = \mathbf{R}_j - \mathbf{R}_i$ is the vector connecting two sites and $\hat{r}_{ij} = \mathbf{r}_{ij}/|\mathbf{r}_{ij}|$. The interaction of the dipole moments may be partly screened through the presence of the ions forming the structural network. Thus the magnitude of the effective moment μ_{eff} may be smaller than the bare moment $\mu = ed/2$ which can be accounted for by the empirical Kirkwood factor g via $\mu_{eff}^2 = g\mu^2$.

We have calculated the partial lattice sums $J_i = \Sigma_j J_{ji}$ for the sites $i = 1 \ldots 4$ in the unit cell and the possible ordered configurations [31]. The sum over j was carried out for a lattice containing 21^3 cells, i.e. $N = 4 \times 21^3$ moments. This large super cell was chosen because the contribution of spins $\boldsymbol{\mu}_j$ a distance r away from $\boldsymbol{\mu}_i$ drops off only as r^{-1}. Using Eq. (12) it is easy to see that the partial dipole sum changes sign only if $\boldsymbol{\mu}_i$ if flipped and (all) $\boldsymbol{\mu}_j$ are held in place. The energetic difference of the two configurations, i.e. the magnitude of the average energy $\langle J\rangle$

required to flip a single spin in an (ordered) lattice is then $|2\Sigma_i J_i/4|$.

The explicit calculation showed that the state of lowest energy compatible with the chosen unit cell is the one depicted in Fig. 1. It is characterized by an anti-parallel alignment of the dipoles with respect to all three spatial directions, i.e. a negative interaction energy $J_0 = -g \times 4950$ K. If one to three spins are flipped with respect to the low energy configuration, then there is a net polarization along at least one of the axes. The average energy of each of the "flipped" configurations is $\langle J \rangle = -(0.28 \pm 0.03)\, J_0$, i.e. positive, indicating a dominance of ferroelectric correlations.

The results presented thus far do not take into account the disorder present in the Al/Si sublattice. However rather than calculating the Coulomb sum over the misbalance of charges in this sublattice [32] it is assumed that the attraction between the negatively charged AlO_4 tetrahedra and the Li^+ charge is comparable to or larger than the dipolar interaction. Then the random occupation of the Al/Si sublattice will lead to random orientations of the dipole moments created by the Li ions in the interstitial pairs. To model this situation we have flipped the orientations of N′ randomly chosen dipoles. Technically speaking we have evaluated the expression $J = 2\Sigma_i P_j J_{ij}$ with the random numbers $P_j = \pm 1$ for a randomly chosen subset of the spins. The quantity $\Delta \equiv N'/N$ can thus be regarded as a measure of the relative strength of what is conventionally called random bonds. In Fig. 2 we show the variances for the distributions $G_\Delta(J)$ obtained by averaging over typically 3000 configurations.

The general behaviour can be well reproduced if only the nearest neighbor interactions are taken into account. Then the interaction energy of a certain spin is essentially given by the probability B_k that k out of the six nearest neighbors are in energetically favorable orientations. If the orientation of the spins is purely statistical, then the variance of the distribution of interaction energies is given by $\sigma_J^2 = (2J)^2 \times [\Sigma B_k k^2 - (\Sigma B_k k)^2]$ with 2J being the distance between two adjacent energy levels and B_k being the

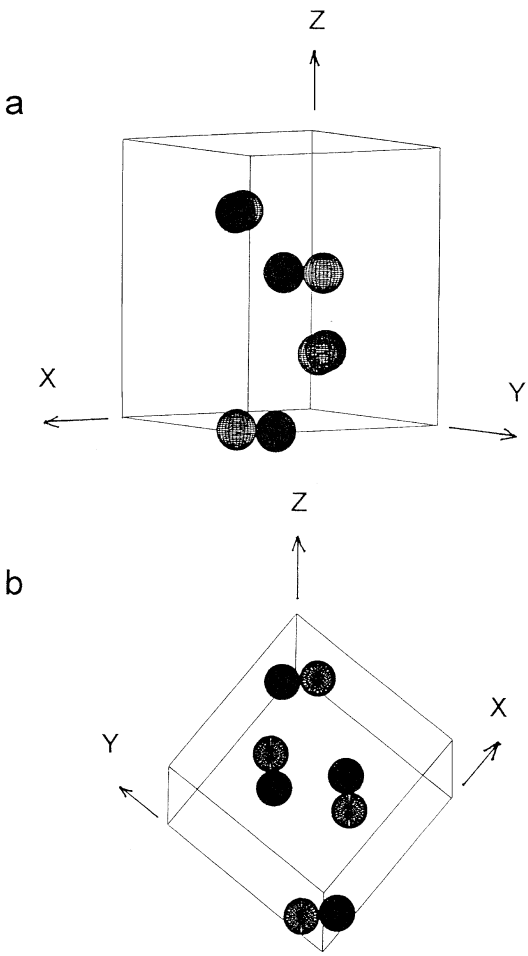

Fig. 1a, b. Possible Li sites in the unit cell of the $P4_32_12$ structure of β-spodumene[2] Part **a** gives a side view, part **b** presents a view from the top. The orientations of the lattice axes X, Y, and Z are indicated. The paired sites give an impression of the orientation of the dipole moments that are responsible for the low-temperature freezing process. The energetically most favorable configuration is symbolized by the different shading which refers to occupied respectively unoccupied sites

Table 1. Positions R_i and moments $\boldsymbol{\mu}_i$ (in units of the lattice constants a = 7.541 Å and c = 9.156 Å, [2] of the configuration schematically shown in Fig. 1. Note that $\boldsymbol{\mu}_2 = -\boldsymbol{\mu}_1$ and $\boldsymbol{\mu}_4 = -\boldsymbol{\mu}_3$. The short hand variables used in the table are $u = (X + Y)/2$, $v = (X - Y)$, and $w = 1 - 2Z$. The Li positions in the unit cell X = 0.0705, Y = 0.1953, and Z = 0.5011 are also taken from [2]

	X/a	Y/a	Z/c
$\mathbf{R}_1$	u	u	1/2
$\mathbf{R}_2$	1 − u	1 − u	0
$\mathbf{R}_3$	1/2 − u	1/2 − u	1/4
$\mathbf{R}_4$	1/2 + u	1/2 − u	3/4
$2\boldsymbol{\mu}_1/e$	− v	v	w
$2\boldsymbol{\mu}_3/e$	v	v	w

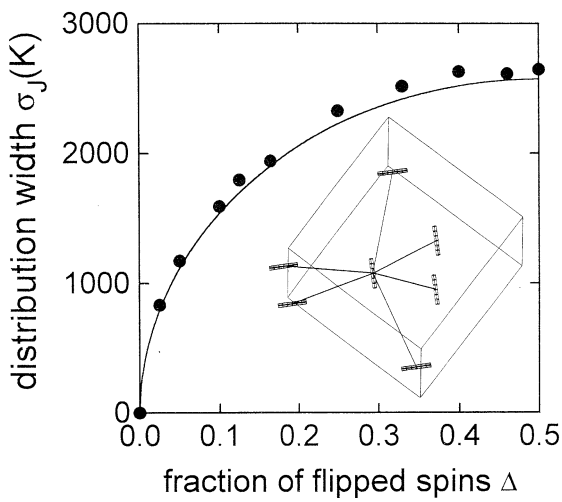

Fig. 2. Standard deviation σ_J (as defined in the text) of the flipping energy distribution versus the "random field" parameter Δ. The dots have been obtained by calculating the dipole sum and averaging over 3000 configurations. The solid line has been calculated using the binomial distribution taking into account the dipolar interactions with the six nearest neighbors of a given pseudo spin, only. The first dipolar coordination shell of a pseudo spin as viewed as in Fig. 1b is shown as inset

binominal distribution $B_k = \binom{6}{k} \Delta^k (1-\Delta)^{6-k}$. The solid line seen in Fig. 2 is calculated using this approach. Good agreement between the simulations and the analytical results is obtained if the interaction energy between two adjacent dipoles is chosen to be $J_{NN} = 1055$ K. In the inset we depict the symmetry of the first coordination shell of a given spin. The good agreement of the simulation on the extended lattice and the analysis in terms of only the nearest neighbor interaction indicates that the contributions of the higher coordination shells effectively cancel.

2.5. Scaling and barrier distributions

The calculations in the previous section can be used to describe the asymmetry $\langle J \rangle$ of the local double well potentials due to dipole-dipole interactions. If for the asymmetry of these double wells one has typically $\langle J \rangle \geq E$, where E is the energy barrier separating the two minima, then a broad distribution in J will lead to a broad distribution in E.

In order to deduce the barrier distribution G(E), Eq. (5) can be used if assumptions concerning the functional form of G(E) are made. Alternatively for energy distributions the imaginary part of Eq. (5) can be rewritten as

$$\varepsilon''(\omega) = \Delta\varepsilon \int \frac{\omega\tau(E)G(E)\,dE}{1 + [\omega\tau(E)]^2}. \tag{13}$$

If G(E) is very broad, i.e. practically independent of E, then the integral can be carried out. If E is expressed using the Arrhenius law

$$E = T \ln \omega_0/\omega \tag{14}$$

then this gives for the distribution of activation energies [33]

$$G(E) = \frac{2\varepsilon''(\omega)}{\pi T \Delta\varepsilon} \tag{15}$$

If a distribution of activation energy is responsible for the broadening of the dielectric loss, it should be possible to scale the data according to the procedure prescribed by Eqs. (14) and (15) [33].

3. Experimental details

Spodumene powder, obtained from Schott Glaswerke, was sintered at 1150°C for several hours and then cooled to room temperature. The material obtained by this procedure contained crystallites with an average diameter of about 30–50 μm and exhibited 84% of the density, 2.37 g/cm^3, of single crystalline spodumene [2]. X-ray powder patterns revealed that our samples crystallize in the space group $P4_32_12$, [2] with no signs of impurity phases. Specimens of plate-like shape were produced for the impedance measurements ($\nu < 1$ GHz), wedge shaped samples were made for the absorptivity investigations in the microwave regime [34]. For the calorimetric experiments, the samples were used in a cylindrical form. Details of the experimental set-up are briefly described elsewhere [19].

4. Results and analyses

4.1. Conductivity relaxation and universal dielectric response (UDR)

The temperature dependence of the electrical conductivity is shown in Fig. 3 for several frequencies. At low temperatures a maximum in σ' is seen which shifts with frequency ν. This behavior is indicative for a dielectric relaxation process and will be dealt with in Sect. 4.2, below. At higher temperatures σ' is due to long range ionic transport. The measurements taken for $\nu < 100$ Hz and $T > 400$ K are independent of frequency and reflect dc behavior. At intermediate temperatures the conductivity is strongly frequency dependent and the shoulders seen near $T = 250$ K indicate a weakly developed relaxation process.

Figure 4 shows the frequency dependence of the electrical conductivity in a double logarithmic representation. At high T and low ν a dc plateau is clearly seen in the data, while for lower temperatures a power law behavior in σ, indicative for ac conductivity, appears to be more pronounced. The solid lines are results from simultaneous fits to $\sigma'(\nu)$ and $\sigma''(\nu)$ using the UDR. A very good description has been achieved in most of the frequency range. However at low temperatures and high frequencies the data vary more strongly than described by the fits. This finding may be due to an approach of constant loss behavior, $\sigma \propto \omega$, at high frequencies. The latter behavior has been found in many ionic conductors and consequently been termed "second universality" [14]. The deviations between data and fits seen at low frequencies and high temperatures are presumably due to blocking electrodes.

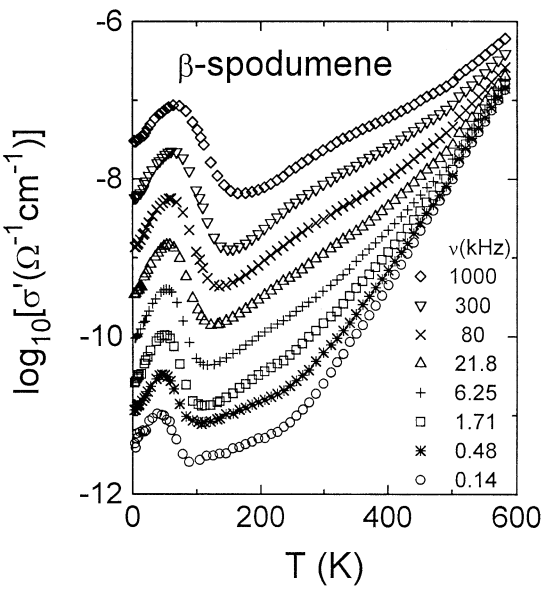

Fig. 3. Temperature dependence of the conductivity σ' of polycrystalline β-spodumene as measured for several frequencies

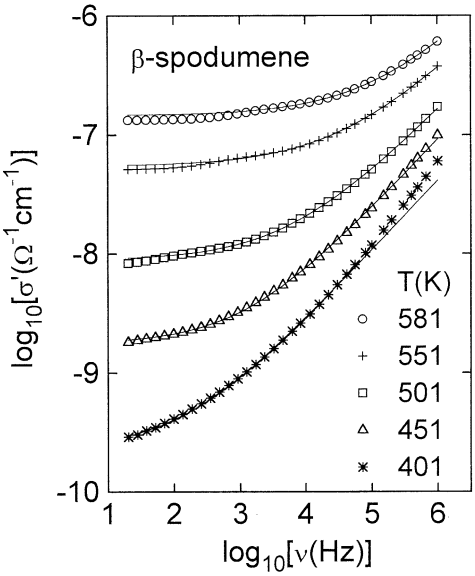

Fig. 4. Frequency dependent electrical conductivity $\sigma'(\nu)$ of β-spodumene. The solid lines are least square fits using the empirical UDR expression (1). Deviation between fits and data at low frequencies and high temperatures are due to electrode polarization effects. Constant loss behavior presumably leads to the slight deviations seen at high frequencies and low temperatures

Real and imaginary parts of the modulus are shown in Fig. 5. The real part exhibits well defined steps. At frequencies at which inflection points appear, the imaginary parts M″ show peaks. The full width at half maximum of these peaks is about 1.8 decades.

The solid lines in this figure are the results of fits of the complex modulus using $M(\omega) = i\omega\varepsilon_0/\sigma(\omega)$ and $\sigma(\omega)$ according to Eq. (1). Again, the agreement is seen to be very good, except at the highest frequencies and the lowest temperatures. Note that the exponents s yielded by this fitting procedure (shown in Fig. 6) are practically identical to those obtained by fitting the conductivity directly. The exponent s increases only very slightly with decreasing temperature.

Figure 7 shows the prefactor A obtained from the fits to $\sigma(\nu)$ and $M(\nu)$ using the UDR in an Arrhenius representation. The appearance of a straight line implies that the ac conductivity is thermally activated with $B_{ac} = 0.37$ eV. Since $s = 0.55 \pm 0.05$ the relation $B_{ac}/B = 1 - s$ predicts B to be (0.82 ± 0.1) eV.

The deviations from power law behavior at high frequencies are most pronounced in a double logarithmic representation of the modulus data. They are shown together with the UDR fits in the upper frame of Fig. 8. Note that the above mentioned minor deviations between data and fits show up at high frequencies and low temperatures as in Fig. 4. The lower frame of Fig. 8 shows the same data with fits using the Fourier-transform of the Kohlrausch function. On the high frequency wing the well known discrepancy [9, 11] between the stretched exponential response and experimental data shows up. The Kohlrausch exponents used to describe the data are shown in Fig. 6 as $1 - \beta$ versus temperature. The value of $1 - \beta$ is slightly temperature dependent and does *not* agree with s.

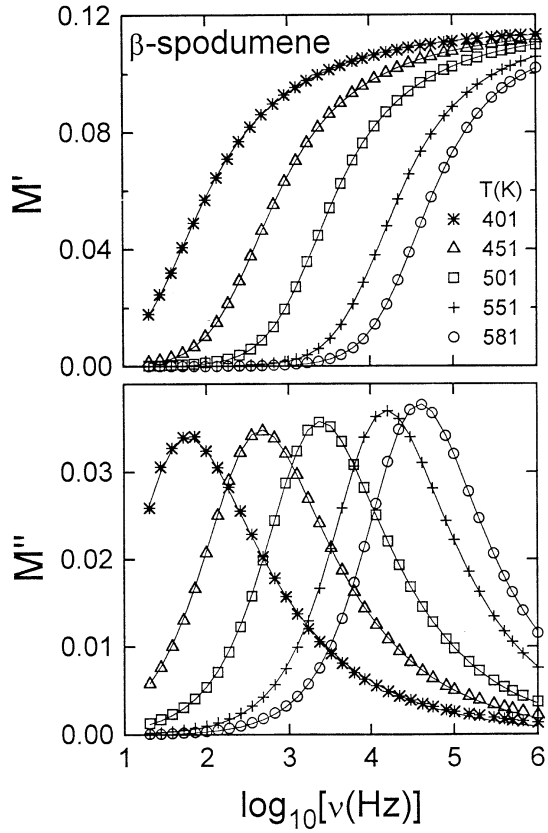

Fig. 5. Real and imaginary part of the complex modulus $M''(\nu)$. The solid lines represents best fits using the universal dielectric response, i.e. $M = i\omega\varepsilon_0/\sigma(\omega)$ with $\sigma(\omega)$ as given by Eq. (1)

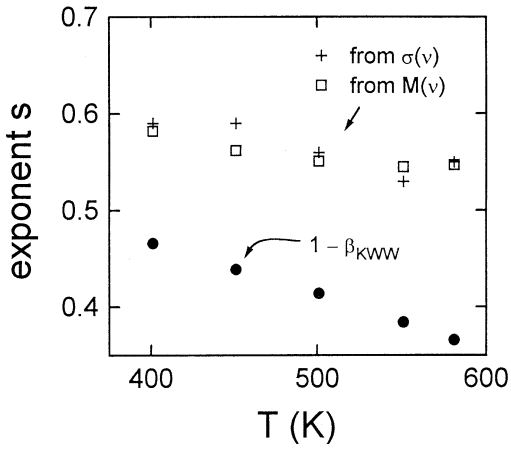

Fig. 6. Parameters characterizing the ionic conduction process plotted versus inverse temperature. The upper frame shows the shape exponents s from the UDR analysis of the impedance data in the conductivity (+) and the modulus (□) representation and the exponent $s = 1 - \beta$ from the Kohlrausch analysis of the modulus spectra (●)

The failure of the Kohlrausch function to give a good fit to the high-frequency wing of modulus (and also of susceptibility) data has been documented many times [11, 35]. But it has been shown that corresponding data often can be superimposed to form a master curve when scaled as suggested by Dixon et al. [36]. As shown in

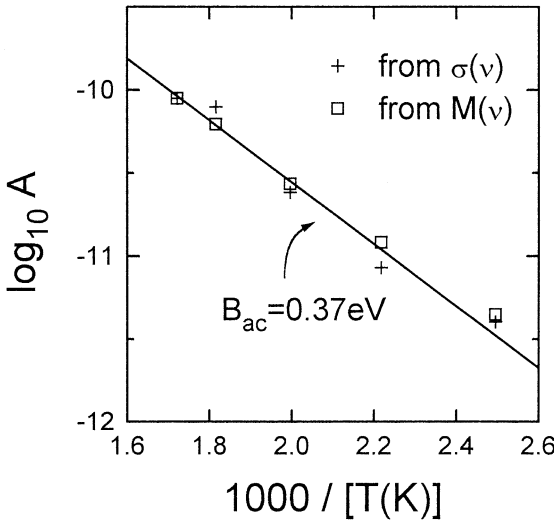

Fig. 7. Prefactor A plotted versus inverse temperature. The analysis of the data in the modulus or in the conductivity give the same effective ac barrier of $B_{ac} = 0.37$ eV

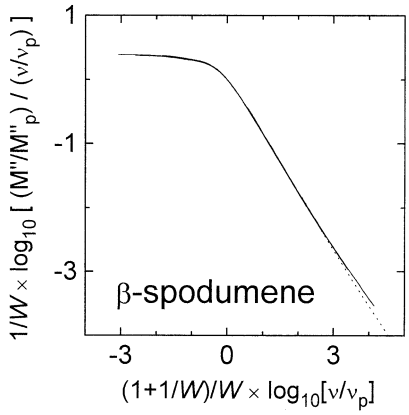

Fig. 9. Same set of data as shown in Fig. 8, but scaled according to the procedure suggested by Dixon et al. with the coordinate axes $X = 1/W \times \log_{10}[(M''/M''_{max}) /(\nu/\nu_P)]$ and $Y = 1/W \times (1 + 1/W) \times \log_{10}(\nu/\nu_P)$. Here W denotes the half width (in decades) of the M'' curves normalized to the Debye width of 1.14 and ν_P is the peak frequency

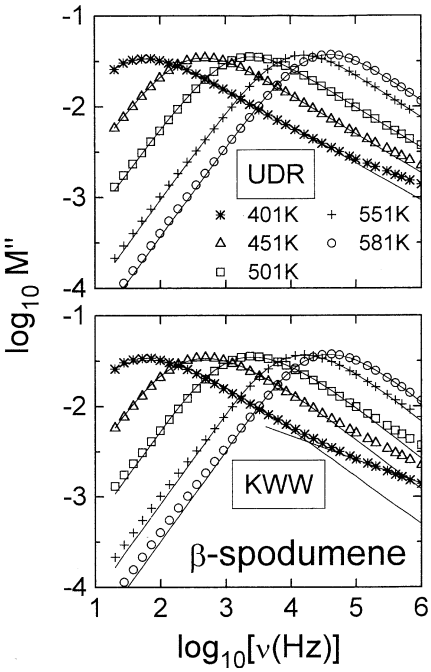

Fig. 8. Double logarithmic plot of the imaginary part of the modulus M″ versus measuring frequency. The solid lines have been calculated using the UDR (upper frame) and the Kohlrausch formalism (lower frame). Both approaches give a good description of the peak region, but systematic deviations on the high frequency wing are clearly seen

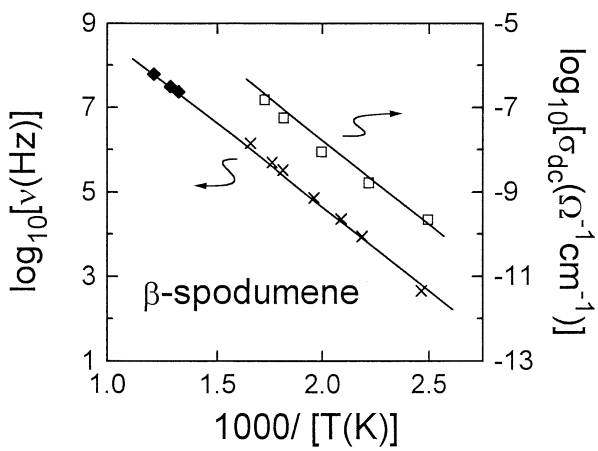

Fig. 10. Arrhenius plot for the conductivity (scale on the right hand side) and characteristic rates obtained from NMR (*) and impedance experiments. The activation energy determined in the present work is in good agreement with that obtained by Munro et al. (×, [3])

Fig. 9 the data for β-spodumene can be scaled on top of one another. However at high frequencies slight deviations from Dixon's scaling *form* show up. It is interesting to point out that even more pronounced deviations from that form have recently be found for a *molten* ionic conductor [37].

Width and time scale parameters obtained from the various fits to the relaxation time data are presented in Fig. 10. The dc conductivity from this work is shown together with results taken from a previous study employing impedance spectroscopy and ^{7}Li-NMR [3]. It is noted that modulus peak frequencies obtained in this work (cf. Fig. 5) differ by about one order of magnitude from those reported in [3]. This apparent discrepancy is likely to be related to the fact that our specimens exhibited lower densities than the single crystalline [21] and presumably also the polycrystalline materials [3, 38] that have been studied earlier. Since $\omega_p \propto \sigma_{dc}$, according to a relation given in Sect. 2.3, lower modulus peak frequencies are expected. The activation energies determined from the various sets of data all agree and yield $B = (0.8 \pm 0.04)$ eV. According to the considerations presented in Sect. 2.2 the carrier density is temperature independent, i.e. the strong electrolyte picture is expected to apply to the case of β-spodumene.

4.2. Freezing in interstitial pairs

In many ionic conductors the low temperature (10 K < T < 100 K) electrical properties are quite featureless [39]. However, β-spodumene is very different in this respect. As Fig. 11 shows the complex dielectric constant as measured for $\nu < 1$ MHz reveals all features of a dipolar freezing process. Above the dispersive regime, the real part of the dielectric constant is independent of frequency in a broad range and the dielectric loss vanishes. This behavior indicates that ac and dc conduction processes due to long-range Li^+ motion is effectively frozen out, and only local relaxations persist.

The magnitude of the dispersion strength $\Delta\varepsilon \approx 2$ gives an important hint concerning the nature of the freezing process. For freely reorienting dipoles $\Delta\varepsilon$ can be expected to be much larger. Since the (bare) dipole moments responsible for the phenomenon are known, the Kirkwood correlation factor $g = 3k_BT/(4\pi\Delta\varepsilon n\mu^2)$ can be calculated. Here n is the density of Li^+ ions [40]. The correlation factor in our case is apparently temperature dependent and in the interval 50 ... 150 K is about $g = 0.1 \pm 0.05$. For non-interacting dipoles one has $g = 1$. Ferroelectric correlations lead to values larger than unity, while antiferroelectric ones are associated with a Kirkwood factor $g < 1$. However the local field corrections, necessary for a quantitative determination of this quantity are hard to evaluate.

The small correlation factor could be due to antiferroelectric interactions among the dipoles that reduce the effective moment, or likewise arise if only a fraction of them participates in the reorientation process. The tendency of the dipoles to align in an antiparallel fashion, anticipated by the calculations presented in Sect. 2.4, is consistent with the observation that the static dielectric constant does obviously not show a hyperbolic T-dependence as would be expected for an ensemble of non-interacting dipoles. The almost constant dispersion step either indicates that a phase transition into an electrically ordered phase takes place at elevated temperatures, which seems quite unlikely, or that the dipole moments associated with the Li ions positions are subject to strong random electric fields that presumably are static in nature.

The decrease of the peak values of the dielectric loss as measured for decreasing frequencies confirms this latter statement concerning the ion freezing process. This is because for $\Delta\varepsilon \approx$ const as suggested by Fig. 11 the loss peak values ε''_{max} should not depend on temperature if the underlying distribution of relaxation times $g(\tau)$, cf. Eq. (5), exhibits a temperature independent width. Thus it can be concluded that $g(\tau)$ broadens significantly on lowering T. Consistent with this statement is the observation made from Fig. 11 that on the high temperature side of the loss peaks, ε'' strongly depends on frequency, while on the low-T wing the dielectric loss is only very weakly frequency dependent. This behavior, which has similarly been made in protonic orientational glasses [33] is often indicative for a broad distribution of energy barriers.

The increase of the peak value ε''_{max} with frequency is by no means restricted to temperatures below the boiling point of liquid nitrogen. Using radio- and microwave frequency experiments, it can be traced all the way up to room temperature and above. Measurements of the dielectric loss carried out at several frequencies in the 1.25–4.35 mm wave region are shown in Fig. 12. As already demonstrated for low frequencies, the dielectric loss

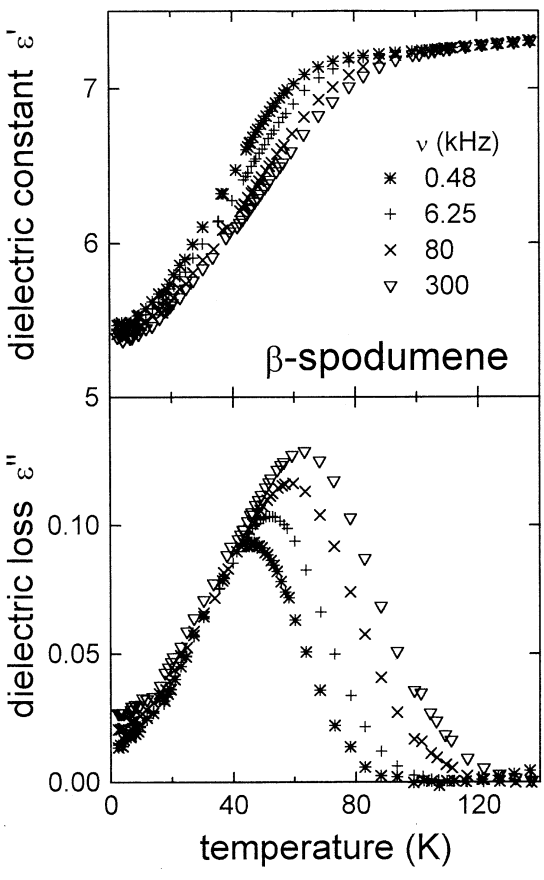

Fig. 11. Temperature dependence of real and imaginary part of the dielectric constant as measured for several frequencies. The frequency dependent dispersion steps and the dielectric loss peaks are characteristic for a dipolar relaxation process. For the lowest temperatures the loss does *not* go to zero and furthermore is slightly frequency dependent

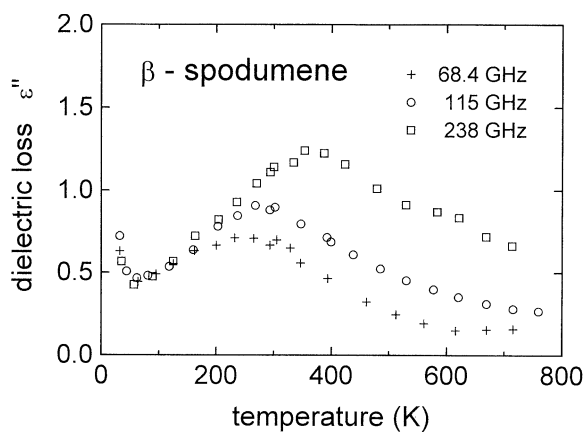

Fig. 12. Dielectric microwave losses of polycrystalline β-spodumene [34]. Note that peak temperature as well as maximum loss increase with frequency

does not seem to extrapolate to zero as $T \to 0$. The negative evidence for the occurrence of a transition into an electrically ordered phase, as inferred from the near temperature independence of $\Delta\varepsilon$ is further validated by the microwave measurements. This is because, at temperatures below about 400 K, the dispersion step cannot be larger than $\Delta\varepsilon_{max} = 2\varepsilon''_{max} \approx 2.5$. The maximum $\Delta\varepsilon$ would be attained if the process leading to the dielectric loss would be governed by a single relaxation time which in view of the shape of the loss curve appears unlikely.

The dielectric loss maxima obtained in the audio-, radio-, and microwave-frequency ranges are shown in an Arrhenius plot, Fig. 13. It is seen that the mechanism underlying the freezing process is thermally activated with an energy of $E_1 = (0.09 \pm 0.02)$ eV. It is interesting to point out that this value coincides with the one given by

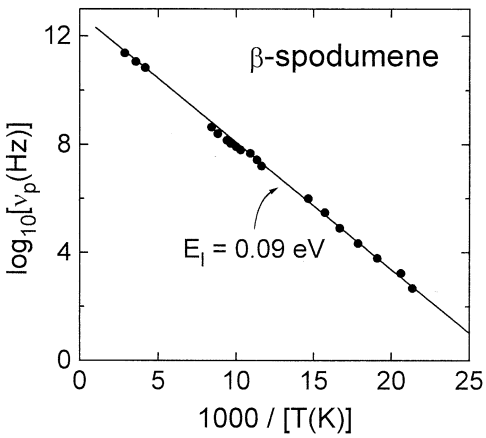

Fig. 13. Arrhenius plot for the loss peak frequencies. The solid line represents an Arrhenius law $\nu_P = \nu_0 \exp(-E_1/k_BT)$ with an attempt frequency $\log_{10}(\nu_0/s^{-1}) = 12.8$ and an energy barrier $E_1 = (0.09 \pm 0.02)$ eV

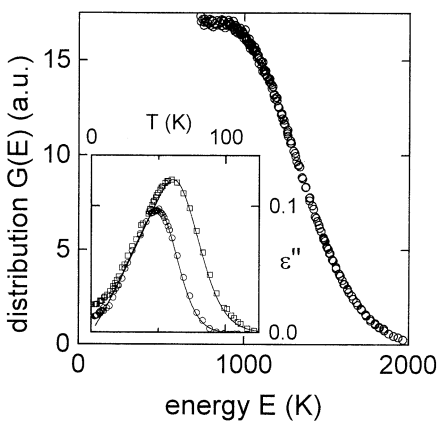

Fig. 14. Distribution of energy barriers G(E) obtained from the dielectric loss according to Eqs. (14) and (15) and using the Arrhenius parameters yielded by the data shown in Fig. 13. A master curve is obtained, indicating that the energy distribution G(E) is temperature independent. The inset shows the dielectric loss calculated for $\nu = 1$ kHz and 100 kHz using G(E) as described in the text. The agreement is excellent except at the lowest temperatures at which an additional absorption mechanism becomes active

Stevels [41] for the motion of a Li^+ ion in the quartz structure.

In order to find the explicit form of the energy barrier distribution, if it exists, we have applied Courtens' scaling procedure [33] to the dielectric loss data. The result of this procedure is shown in Fig. 14. It is seen that all data scale on a master curve. The distribution of energy barriers according to this plot is seen to be constant up to about $E = 1000$ K and then drops off like a Gaussian with a half width at half maximum of 380 K. In order to achieve scaling it is found that $\Delta\varepsilon$ is required to be temperature independent at least down 25 K. As a cross check, the barrier distribution just described has been used to calculate the dielectric loss. The result of these calculations together with the experimental data is shown as inset in Fig. 14. The agreement is excellent except at low temperatures for which Eq. (15) predicts $\varepsilon'' \propto T$. It appears likely that at low temperatures tunneling processes, which we have neglected so far, but which are a generic feature of dynamics associated with asymmetric double well potentials [42] provide an absorption mechanism which is responsible for the deviations seen for $T \to 0$.

5. Discussion

One of the most surprising findings of this work is that the freezing of the Li^+ ions proceeds in an orientational glass (OG) like fashion. Hence it may be interesting to discuss the similarities and the differences to conventional OG. The first question concerns the freezing process itself. It is usually characterized by thermally activated average relaxation rates [43, 44]. The rates show a wide distribution which broadens considerably on approaching the OG transition [33, 45, 46]. Both features are also observed in β-spodumene. Anomalous low temperature properties and particularly an anomalous low temperature specific heat are an additional characteristic of structural and orientational glasses.

In order to check the properties of β-spodumene also in this respect we have carried out a calorimetric investigation using the adiabatic Nernst method. In Fig. 15 we

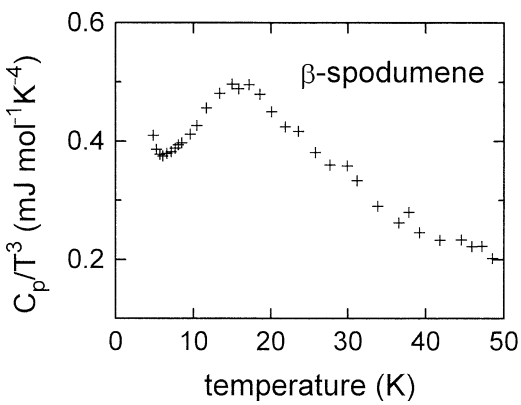

Fig. 15. Low temperature specific heat of β-spodumene. The data are presented as C_P/T^3 versus T in order to emphasize the deviations from Debye behavior ($C_p \sim T^3$)

show the measured specific heat C_P of β-spodumene in a representation of C_P/T^3 vs. T. The hump seen in the 10–20 K range, typical for amorphous solids, [47] and the local minimum due to the linear term in C_P at the lowest temperatures are both observed for β-spodumene.

Another important issue for the understanding of the dynamics of OG concerns the role that is played by random bonds, which are due to the mutual interactions of the freezing moieties, in relation to the role played by the random fields which are due to the coupling of the pseudo-spins to the underlying center of mass lattice [48]. This kind of disorder in conventional OG is due to the fact that OG are *always* mixed crystals [49]. Although β-spodumene is a single phase material, it is clear that in this crystal the random fields stem from the disorder in the Al/Si sublattice. These random fields couple to the position of the Li ions through Coulombic interaction forces. It is however interesting to note that random fields alone do not give rise to glassy low temperature properties [50]. Therefore the influence of the random bonds, though hard to evaluate on the basis of the present data, have also to be taken into account.

Likewise, quantitative conclusions concerning the strength of the random fields are difficult to draw. On the one hand the width of the experimentally determined distribution of energy barriers is much smaller than that suggested by the calculations presented in Sect. 2.4 for the case of $\Delta = 0.5$. On the other hand calculations are to be rescaled by the effective screening of the bare dipole moments. However, it is not clear whether the Kirkwood correlation factor g determined from the magnitude of the dispersion step is entirely due to screening effects. The relatively small (and furthermore obviously temperature dependent) value of g rather seems to indicate that on lowering the temperature an increasing number of dipoles freeze in. The quasi-static freezing of orientational degrees of freedom already at large temperatures (with respect to a potential spin-glass transition temperature) as implied also by the microwave data, are a hallmark of random field dominated systems. In order to obtain numerically reliable estimates of the random field parameter Δ it is clear that further work is needed using local probes. In this respect magnetic resonance experiments have previously been shown to be useful [51].

In the following we briefly discuss some results of our conductivity studies which are summarized in Fig. 6, where we have plotted the temperature dependence of the exponent s obtained by fitting the data in the conductivity and in the modulus formalisms. At first glance it may appear surprising that the exponent s extracted from the same data shows systematic and significant deviations from $1 - \beta$. But obviously the various ways of fitting the same set of data are particular sensitive to data in different frequency ranges. This statement together with the observation that several power laws exist for frequency ranges $\omega > \omega_C$ or $\omega > \omega_{peak}$ (cf. Fig. 6) explains why it is so difficult to extract reliable exponent parameters. It is important to note that this conclusion not only applies to the case of β-spodumene. This is because high frequency deviations from the $\sigma' \propto \omega^s$ or $M'' \propto \omega^{-(1-s)}$ behaviors are a generic feature of most ionic conductors, as extensively discussed in the literature [11–14].

6. Conclusions

We have investigated two aspects of the motion of Li^+ ions in β-spodumene. At low temperatures (or very high frequencies) localized relaxational excitations show up. At high temperatures thermal activation of the mobile ions leads to long ranged charge transport. The main result from our conductivity study is that the non-existence of a well-defined power law regime for frequencies above the characteristic one does lead to ambiguities in the analysis when carried out in the framework of existing formalisms. The scaling form suggested by Dixon et al. is traced only approximately, obviously because in β-spodumene, as in many other ionic conductors, a constant loss behavior is seen at high frequencies.

The freezing of the Li ions in the interstitial double well potentials provided by the peculiar structure of β-spodumene has been studied experimentally and also using a simple model focusing on the dipolar interaction between the pseudo spins associated with these "off-center" ions. The calculations showed that in the absence of disorder the dipolar interaction would lead to an antiferroelectrically ordered configuration. The random occupation of the Al/Si sublattice is schematically taken into account by introducing a random-field parameter Δ, which controls the width of the distribution of interaction energies.

Using a scaling procedure suggested by Courtens, [33] a broad energy barrier distribution is identified to be responsible for the shape of the dielectric loss peaks. The mean energy barrier required to perform the scaling analysis has been determined from dielectric loss measurements covering the kHz to THz range and was found to be $E = 0.09 \pm 0.02$ eV. According to the calculations presented in Sect. 2.4 this is about equal to the interaction energy J supporting the notion that many aspects of the dipolar dynamics can be explained by the existence of asymmetric double well potentials. The broad distribution of barrier heights (as well as asymmetries) and the temperature dependence of the static susceptibility (which is proportional to the dispersion step $\Delta\varepsilon$) indicate that the random electric fields introduced by the disorder in the Al/Si sublattice have a major impact on the orientational glass transition in β-spodumene.

Dr. Franz Drexler has generously supplied the microwave data. Dr. W. Pannhorst from Schott Glaswerke, Mainz, is thanked for a fruitful collaboration on aluminosilicates. We gratefully acknowledge the support of this project by the Deutsche Forschungsgemeinschaft (SFB 262-D5).

References

1. Aitken, B., Beall, G.: In: Material Science and Technology. vol. 11, p. 269 Cahn, R.W. Haasen, P., Kramer, E.J. (eds.) Weinheim, VCH:1994; Bach, H., (ed.); Low Thermal Expansion Glass Ceramics, Berlin: Springer 1995
2. Li, C.-T., Peacor, D.R.: Z. Kristallogr. **126**, 46 (1968)
3. Franke, W., Heitjans, P.: Ber. Bunsenges. Phys. Chem. **96**, 1674 (1992); Munro, B., Schrader, M., Heitjans, P.: Ber. Bunsenges. Phys. Chem. **96**, 1718 (1992); Franke, W., Heitjans, P., Munro, B., Schrader, M.: In: Proceedings of the International Conference on Defects in Materials Singapore: World Scientific, 1992

4. For reviews see,: Angell, C.A.: Chem. Rev. **90**, 523 (1990); Hunt, A.: J. Non-Cryst. Solids **160**, (1993)
5. Almond, D.P., West, A.R.: Nature (London) **306**, 456 (1983)
6. Long, A.R.: Adv. Phys. **31**, 553 (1982); Elliott, S.R.: Adv. Phys. **36**, 135 (1987)
7. Jonscher, A.K.: Nature **267**, 673 (1977); Hill, R.M., Jonscher, A.K.: Contemp. Phys. **24**, 75 (1983)
8. Dyre, J.C.: J. Appl. Phys. **64**, 2456 (1988); J. Non-Cryst. Solids **135**, 219 (1991)
9. Macedo, P.B., Moynihan, C.T., Bose, R.: Phys. Chem. Glasses **13**, 171 (1972)
10. Ngai, K.L. In: Non-Debye Relaxation in Condensed Matter. Ramakrishnan, T.V. (ed.) Singapore: World Scientific, 1987
11. Moynihan, C.T.: J. Non-Cryst. Solids **172–174**, 1395 (1994)
12. Elliott, S.R.: J. Non-Cryst. Solids **170**, 97 (1994)
13. Johari, G.P., Pathmanathan, K.: Phys. Chem. Glasses. **29**, 219 (1988); Parthun, M.G., Johari, G.P.: J. Chem. Soc. Farady Trans. **91**, 329 (1995)
14. Nowick, A.S.: J. Non-Cryst. Solids **172–174**, 1389 (1994)
15. Höchli, U.T., Knorr, K., Loidl, A.: Adv. Phys. **39**, 405 (1990)
16. Loidl, A., Böhmer, R.: In: Disorder on Relaxational Processes p. 659. Richert, R., Blumen, A. (eds.) Berlin: Springer 1994
17. Phillips, W.A. (ed.),: Amorphous Solids: Low Temperature Properties Berlin: Springer 1980
18. Böhmer, R., Gerhard, G., Drexler, F., Loidl, A., Ngai, K.L., Pannhorst, W.: J. Non-Cryst. Solids **155**, 189 (1993)
19. Böhmer, R., Lotze, M., Lunkenheimer, P., Drexler, F., Gerhard, G., Loidl, A.: J. Non-Cryst. Solids **172–174**, 1270 (1994)
20. Lunkenheimer, P., Drexler, F., Gerhard, G., Böhmer, R., Loidl, A.: Z. Naturforsch. A (in press)
21. Roth, G., Böhm, H.: Solid State Ionics **22**, 253 (1987)
22. Angell, C.A.: Annu. Rev. Phys. Chem. **43**, 693 (1992)
23. Note that in certain models even forward and backward hops are correlated, see Funke, K., Hoppe, R.: Solid State Ionics **40–41**, 200 (1990)
24. Lidiard, A.B.: In: Handbuch der Physik vol. 20, p. 246, Flügge, S., Berlin: Springer, 1957
25. Pechenik, A., Susman, S., Whitmore, D.H., Ratner, M.A.: Solid State Ionics **18&19**, 403 (1986); Ishikawa, T., Ishii,T.: J. Phys. Soc. Jpn. **61**, 4484 (1991)
26. see e.g., Fusco, F.A., Tuller, H.L.: In: Superionic Solids and solid Electrolytes Laskar, A.L. (ed.) London: Academic Press, 1989
27. The relation due to Barton, Nakajima, and Namikawa has been discussed in [4, 8]
28. Note that the assumption that E_n depends linearly on temperature is formally equivalent
29. It has to be noted that many other representations of conductivity data are known, e.g. in the form of complex impedance, resistivity, admittance, etc. plots. For a recent example of the direct measurement of the electrical modulus, see Wagner, H., Richert, R.: Polymer (submitted)
30. Williams, G., Watts, D.C.: Trans. Faraday Soc. **66**, 80 (1970)
31. In fact only 8 configurations need to be considered for a unit cell since J_{ij} as given by Eq. (12) does not change if $\boldsymbol{\mu}_i$ and $\boldsymbol{\mu}_j$ are flipped simultaneously
32. This problem is analogous to the well known calculation of Madelung constants which due the weaker drop-off of the interaction strength however is more intricate than the calculation of dipole sums
33. Courtens, E.: Phys. Rev. B **33**, 2975 (1986); Brückner, H.J., Courtens, E., Unruh, H.-G.: Z. Phys. B **73**, 337 (1988)
34. Drexler, F.: Dissertation, (Universität Mainz, 1992)
35. Chamberlin, R.V.: Phys. Rev. B **48**, 15638 (1993)
36. Dixon, P.K., Wu, L., Nagel, S.R., Carini, J., Williams, B.D.: Phys. Rev. Lett. **65**, 1108 (1990)
37. Lunkenheimer, P., Pimenov, A., Kohlhaas, R., Böhmer, R., Loidl, A.: (unpublished)
38. We thank Prof. Heitjans for a useful conversation concerning this issue
39. Lim, B.S., Vaysleyb, A.V., Nowick, A.S.: Appl. Phys. A **56**, 8 (1993)
40. The density can be calculated using the lattice parameters given in Table 1 to be $n = 4/(a^2c) = 7.68 \times 10^{21}\ cm^{-3}$
41. Stevels, J.M.: J. Non-Cryst. Solids **40**, 69 (1980)
42. Kanert, O., Küchler, R., Dieckhöfer, J., Lu, X., Jain, H., Ngai, K.L.: J. Non-Cryst. Solids **172–174**, 1277 (1994)
43. van der Klink, J.J., Rytz, D., Borsa, F., Höchli, U.T.: Phys. Rev. B **37**, 89 (1983)
44. Hutton, S.L., Fehst, I., Böhmer, R., Mertz, B., Braune, M., Lunkenheimer, P., Loidl, A.: Phys. Rev. Lett. **66**, 1990 (1991)
45. Xhonneux, P., Courtens, E., Grimm, H.: Phys. Rev. B **38**, 9331 (1988)
46. Ries, H., Fehst, I., Böhmer, R., Loidl, A.: Z. Phys. B (in press)
47. It has to be noted that excess contributions have been reported also for other crystalline ionic conductors, Gmelin, E., Villar, R.: Physica B **108**, 1003 (1981)
48. Michel, K.H.: Z. Phys. B **68**, 259 (1987); Binder, K., Reger, J.: Adv. Phys. **41**, 547 (1992)
49. To avoid confusion here we point out, that also *pure* supercooled orientationally disordered crystals are sometimes termed OG. A clear distinction of the two classes of crystals has been given in [16]
50. Cahill, D.G., Watson, S.K., Pohl, R.O.: Phys. Rev. B **46**, 6131 (1992) present the thermal conductivity of KBr-KCl mixed crystals which shows no glass-like features and discuss other examples, see also Watson, S.K.: Phys. Rev. Lett. **75**, 1965 (1995)
51. Blinc, R., Dolinsek, J., Pirc, R., Tadic, B., Zalar, B., Kind, R., Liechti, O.: Phys. Rev. Lett. **63**, 2248 (1989)